Comparison and evaluation of recently reported methods for optimization of industrial drying regimes

To cite this article: M Vasic and Z Radojevic 2018 *IOP Conf. Ser.: Mater. Sci. Eng.* **400** 062030

IOP Conf. Series: Materials Science and Engineering **400** (2018) 062030 doi:10.1088/1757-899X/400/6/062030

Comparison and evaluation of recently reported methods for optimization of industrial drying regimes

M Vasic and Z Radojevic
"Institute for testing of materials", Bulevar vojvode Mišića 43 1100 Belgrade, Serbia

E-mail: milos.vasic@institutims.rs

Abstract. In our previous studies we have presented the calculation method along with the procedure for setting up the non isothermal drying regime. Even though this method is harmonized, with the theory of moisture migration during drying and can be used to predict the optimal industrial drying regime and proper drying air parameters, up till now it was not compared with other models. The main goal of this paper, was to compare and evaluate our model with the one reported by the German group of authors in 2008. The first task was to create criteria for model evaluation. Five parameters were chosen: non-existence of cracks, total drying time, twist coefficient, chamber coefficient and flexural strength. The second task was to create a software tool, for modeling the first and second drying section of green clay masonry element, using the instructions provided within the published articles. The third task was to apply German and our procedure on the same clay raw material. Results have shown the absence of cracks on dried and fired samples. In the case of German method total drying time, as well as twist and camber coefficients were higher while the physico - mechanical properties were lower. Presented results have additionally validated that our dying model can be used for the accurate prediction of industrial drying kinetics and a reliable estimation of moisture transport during drying.

1. Introduction

Drying is highly energy-intensive process, due to the fact that it is necessary to supply the latent heat of evaporation to remove the water from the drying object. Any energy saved in the drying process has positive impact on the environment and the production costs reduction. This is a challenging task which is associated with the real thermodynamic barriers. During drying the moisture contained within the green clay masonry element is removed. If the moisture content is not removed adequately severe stresses will arise inside the product. This will lead to cracking and consequently the reduction of the final products quality. Since the quality of the final clay masonry elements is directly related with the drying process many researchers are focused on the drying analysis. Factors that are correlated with the drying rate and the simultaneous mass and heat transfer process are divided in two groups: external and internal. External factors are drying air temperature, humidity and velocity. Internal factors, usually called thermodynamic factor, are dictating which mechanisms of moisture transport, from the interior of the masonry unit up to its surface, will be active during drying. These factors are closely related with the raw material clay content, pore size distribution, pore volume, capillarity, and clay plasticity [1,2].

In order to properly describe industrial drying regime it is necessary to analyze both the external and internal moisture transport. This can be achieved at four complexity levels: diffusion [3-5], receding [6,7], macroscopic-continuum [8,9] and pore-network [10]. Each level uses different

modeling approach and conjugate modeling degree, which is determined by the way in which the heat and mass transport in air are accounted for in the calculation procedure.

German group of authors has reported the procedure for modeling the first and second drying section of green clay masonry elements [2,11,12]. According to those authors at the beginning of drying the moisture diffusion coefficient is proportional to the square of the moisture fraction until the end of shrinkage. After the end of shrinkage the resistance for the moisture transport up to the surface of the green masonry unit is increased due to the penetrating air. This is correlated with the sharp drop of the moisture diffusion coefficient value. This model can predict the moisture transport on the basis of the moisture and temperature dependent moisture diffusion coefficient k. They proposed differential equation (1) for determination of the moisture conduction (diffusion) inside the wet masonry clay unit.

$$\frac{d\psi}{dt} = \frac{\partial}{\partial z}\left(k(\psi, \theta)\frac{\partial \psi}{\partial z}\right) \quad (1)$$

Ψ – volumetric local water content; z – length of the masonry unit; t – time; ϴ – temperature

In the first drying section the initial water content, which is constant over the cross-section, defines the initial conditions while the coupled heat and mass transfer to the surface of the green product defines the peripheral condition necessary for the numerical solution. In the second drying section these authors used equation (2) for determination of the vapor diffusion through the dried porous layer.

$$\dot{m}_d = -\frac{D}{\mu S_{tr}}\frac{p}{R_d T} ln\frac{p-p_{DO}}{p-p_{DK}} \quad (2)$$

$\dot{m}_d$ - steam mass flow density flowing through the dry shell; D – diffusion coefficient of water vapor in air; μ - diffusion resistance coefficient; S_{tr} – momentary distance of the drying plane from the surface of green product; Rd – special gas constant; T – absolute temperature within the dry shell; p – total pressure; p_{DO} – steam pressure at the surface; p_{DK} - steam pressure at the drying plane (identical with the saturation steam pressure at the plane temperature).

The procedure for setting up the non isothermal drying regime, that is consistent with the theory of moisture migration during drying, was recently reported [13,14]. In order to properly apply this procedure it is necessary to firstly determine the change of effective moisture diffusivity vs. moisture content or drying time (Deff – MR or Deff - t curve) for each isothermal experiment. These plots represent a good indicator for evaluation and presentation of the overall mass transport property of moisture during isothermal drying. All mechanisms of moisture transport and their transition from one to another during isothermal drying, within a green clay masonry element, are visible on previously mentioned plots. Detailed information regarding the procedure for identification and quantification of moisture transport and their transition during drying can be found in reference [1]. Optimal drying regime is consisted of five isothermal segments. Durations of previously mentioned drying segments were detected from the relevant Deff – MR curves.

2. Materials and Methods

The raw material, used in this study, was obtained from the Serbian roofing tile producer. Its detail characterization was reported in the study [15]. The raw material was first dried at 600C and then crashed down in a laboratory perforated rolls mill. After that simultaneously it was moisturized and milled in a laboratory differential mill, first with a gap of 3 mm and then of 1 mm. Laboratory roofing tile samples 120 × 50 × 16 mm were formed, from the previously prepared clay, in a laboratory extruder "Hendle" type 4, under a vacuum of 0.8 bar. Two experimental procedures were applied on the previously formed roofing tiles.

The first one, called German, was identical to the procedure reported in article [11]. According to this method several formed roofing tiles with the exception of the facing surface were enclosed and thermally insulated on all other sides. Prepared samples were put into the drying chamber. The air parameters inside the chamber were, registered before the samples were put inside and afterwards

were regulated with accuracies of ±0.2 °C, ±0.2 % and ±0.1 % for temperature, humidity and velocity, respectively. The total water mass flow leaving the formed units through the face surface was continually monitored and recorded during drying. The mass, linear shrinkage and the temperature of the samples were continuously registered with the accuracies of 0.01 g, 0.2 mm and 0,2 °C. The limiting moisture content was calculated using the using the equation (3).

$$\psi_1 = [\psi_0 - (1 - (1 - \xi^3)]\frac{\rho_{SE}}{\rho_0} \quad (3)$$

ξ - Final shrinkage degree; ψ_0 - initial water fraction, ρ_{SE} – density of the dry solid, ρ_0 - initial density of the wet masonry unit.

When the moisture profile, in which all moisture contents were still higher than the limiting one, was established the specimens were cut into slices. All cut slices were put together and drying was continued. Dry mass of the every individual slice was measured just after the drying was over. That has allowed us to experimentally determine the moisture gradient (distribution) along the length of the roofing tile.

Using the instructions provided within the published articles [2,11,12] a software, for modeling the drying process, according to the German method was designed. The fact that the water mass flow leaving the roofing tile is proportional to the moisture gradient at its surface was used. The moisture diffusion coefficient kR, for the referenced water content at room temperature, was easily computed using the previously experimentally established moisture gradient data set. It is important to mention that up to the limiting moisture content ψ1, the solid particles moves closer together as they lose the enveloped water until the contact between them is reached. This point represents the end of shrinkage. Further loss of volume is compensated by the air penetrating into the pore system of the green masonry unit [11]. That is the reason why two equations were used for determination of the moisture diffusion coefficient k for any selected water content at room temperature. If selected water content value ψ was above the limiting moisture content ψ1 then the equation (4) was applied. Equation (5) was valid for any selected ψ value lower than the limiting ψ1. The next step was to determine the moisture diffusion coefficient for any temperature within the range starting from 250C up to the 900C. Relation (6), was implemented in the software, and used for calculation of temperature dependent moisture diffusion coefficient.

$$k = k_R(\frac{\psi}{\psi_R})2 \quad \text{if the } \psi \geq \psi 1 \quad (4)$$

$$k = k_R(\frac{\psi_1}{\psi_R})2\ 107(\psi\text{-}\psi 1) \quad \text{if the } \psi \leq \psi 1 \quad (5)$$

$$k(\theta) = k(25°C)(1 + 0{,}0225(\frac{\theta}{°C} - 25)) \quad (6)$$

Theoretically the drying rate is described as the mass flow density $\dot{m}$ of the water evaporating from the surface of the formed roofing tile. In the first drying section the entire heat flow $\dot{q}$ which is transferred to the formed roofing tile is used entirely for the evaporation of water. This means that the heat flow density is proportional to the mean hat transfer coefficient α and the difference between the temperature of the air surrounding the formed roofing tile and the cooling limit temperature which has the same value as the formed roofing tile temperature at the beginning of the drying. In the second drying section the heat flow density is used mainly as evaporation enthalpy and partly as energy used for heating the clay roofing tile. Equation (7), for calculation of the heat flow density during the second drying section, was implemented in the software. It was assumed that the temperature increase in the roofing tile during drying is equal to the increase registered in its centre. The temperature of the wet part of the roofing tile was assumed to be constant.

$$\dot{q} = \dot{m} \cdot r + (\rho_d \cdot c_d + \psi(t) \cdot \rho_w \cdot c_w) \cdot \frac{s}{2} \cdot \frac{dT_c}{dt} \quad (7)$$

r – enthalpy, ρ_w– water density, c – specific heat capacity, d – roofing tile thickness, T_c – temperature in the center of the roofing tile.

The second experimental procedure was reported in article [13,14,16]. According to this method the formed roofing tiles were first packed into plastic bags which were afterwards sealed and put into a glass container with lid. This was done to prevent the moisture content fluctuations within the stored samples. Prepared samples were than isothermally dried in the laboratory recirculation dryer. The mass of the samples and their linear shrinkage were continually monitored and recorded during drying. The accuracies of these measurements were 0.01 g and 0.2 mm. Drying air parameters were regulated inside the dryer with accuracies of ±0.2 °C, ±0.2 % and ±0.1 % for temperature, humidity and velocity, respectively. Series of isothermal drying curves were reordered.

This method is harmonized with the theory of moisture migration during drying. According to this theory effective diffusivity - moisture content (Deff – MR) curves are used for identification of all active mechanisms of moisture transport and their transitions during isothermal drying. Identified drying segments as well as the corresponding active mechanisms up to the "lower critical" point F are summarized according to the reference [1] in the table 1.

Table 1. Possible drying mechanisms up to the "lower critical" point F according to reference [1].

Drying segment	Transport of liquid water	Transport of vapor
A B	Capillary pumping flow (CPF) through the biggest capillaries	/
B C	CPF through macro capillaries, HF	/
C D	CPF through mezzo capillaries, HF	/
D E	CPF (from capillaries in funicular state),HF and liquid diffusion in the pores	hydrodynamic flow (HF)
E F	Creeping along the capillary when the liquid is in the funicular state or by the successive evaporation – condensation mechanism between liquid bridges.	HF (difference in total pressure)

0A - Initial period / AE - Constant period / FL - Falling period / D - "upper critical" point; "funicular state" – continuous threads of moisture are present in the pores. Surface is completely wet; Drying front start to recede into body / DE – Partially wet surface / F - "lower critical" point; "pendular state" – continuous threads of moisture are not present in the pores; "last" wet patches has disappeared from the surface.

Proposed drying regime was consisted of five isothermal segments. Durations of the first four drying segments were detected from the relevant Deff – MR curves. Duration of the fifth segment was determined experimentally. The first four segments were specified as the intervals OC, CD, DE and EF on the corresponding Deff – MR curves.

Roofing tiles samples which remained after drying, using both presented experimental procedures, were gathered and afterwards dried to constant mass. Dried samples were heated in oxygen atmosphere with the heating rate of 1.4^0C/min from room temperature up to 610^0C, and further with the heating rate of 2.5^0C/min up to the 1050^0C. Samples were kept at 1050^0C for 2 hours. Flexural strength was determined on dried (DS) and fired samples (FS) using the procedure given in EN 538 norm. Twist (TC), longitudinal camber (RL) and transverse camber (RT) coefficients were determined on fired samples using the procedure described in EN 1024.

3. Results and discussion

Previously presented German procedure was firstly used to predict the dependence of moisture diffusion coefficient with water content at 25^0C. After that the time dependent moisture content during

drying was calculated along with the corresponding simulation of the drying process. Measured data used as model inputs are specified in the table 2. Modeling results are presented in the figure 1.

Table 2. Experimentally determined model inputs.

Density of dried mass in kg/m^3	1810
Initial moisture content in kg/kg ref. to.dry	0.208
Thickness of the green (formed) sample in mm	16
Temperature of the green sample at the dryer entrance in ^{0}C	25
Linear shrinkage in %	6.60
Moisture diffusion coefficient k_R in 10^{-9} m^2/s determined experimentally at 20^{0}C using the samples with initial moisture content 0,196	9.0
Diffusion resistance coefficient of dry mass	8
Heat conduction coefficient of dry plate in W/(mK)	0.5
Heat transmission coefficient in W/(m^{2}K)	17
Initial (air temperature) ^{0}C	45
Relative humidity of Initial air in %	75

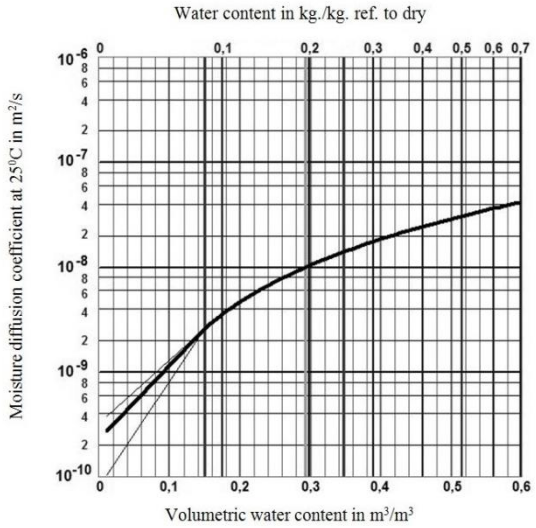

Figure 1a

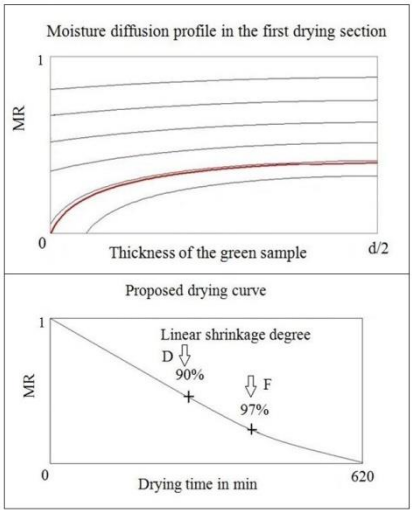

Figure 1b

Figure 1. Outputs from the software created according to the German modelling procedure.

It can be seen that the limiting water content at 25^{0}C in kg/kg ref.dry was 0,079 (fig.1a). This value is similar to the critical moisture content reported in the table 5 [14]. Fig.1.b is divided into two partial pictures. Moisture profiles established inside the roofing tiles, during the first drying segment, are presented at every 70 minutes in the upper partial picture. The left-hand edge of this partial picture represents the surface of the green roofing tile, while the right-hand edge represents the green roofing tile plane symmetry. It can be seen that the area between two neighboring moisture profiles up to the red curve have equal size. This is expected because the drying rate is constant in the first drying period. Simulated drying curve is presented in the second partial picture. Two marks can be seen on this curve. These marks are representing the moments when the linear shrinkage has reached 90 and 97% respectively. According to the theory of moisture movement during drying the first marks is also representing the "upper critical" point D while the second one is representing the "lower critical" point F. These points are reached after 277 and 395 min respectively. First drying segment is over after 320 min, when the characteristic point E is reached. The transition drying segment is located between the

points E and F. It is a common industrial practice to increase the temperature inside the dryer, from the end of the first drying segment, with the rate of approximately 5-10 ^{0}C/h. The drying air temperature was increased, in this simulation, after 320 min using the 10 ^{0}C/h rate. This rate was kept until the temperature in the centre of the drying roofing tile did not reached 68^{0}C. Due to this temperature rise, the drying rate in the second drying segment was prevented from dropping to low. Total drying time in this simulation was 620 min.

Experimental conditions presented at table 3 and 5 were used to set up the drying regime according to the second presented procedure. Even though the cracks were registered during drying in the experiment 5, the exact position of all characteristic drying points (CDP) were calculated. The calculation procedure "CRP", for prediction of the CDP for cracked samples, described in reference [14] was applied. CDP points registered on the relevant Deff – MR curves, for all isothermal experiments up to the point F, are summarized in table 4. Physico - mechanical properties of the dried and fired roofing tiles are summarized in the table 6 and 7.

Table 3. Drying air parameters used in isothermal experiments.

Experiment	Air velocity, W (m/s)	Air humidity, V / %	Air temperature, T / °C
1	3	80	42
2	1	70	45
3	2	63	40
4	2	63	45
5	2	63	50*

*Cracks were detected during drying

Table 4. Values in the characteristic points (marks) up to the point F.

Exp.		1	2	3	4	5
A	t (min)	45	35	19	16	14
	MR	0.985	0.991	0.975	0.976	0.973
B	t (min)	141	87	51	49	44
	MR	0.845	0.874	0.864	0.868	0.865
C	t (min)	200	168	83	75	69
	MR	0.695	0.725	0.760	0.763	0.761
D	t (min)	330	257	136	125	110
	MR	0.535	0.565	0.595	0.604	0.605
E	t (min)	450	325	181	168	152
	MR	0.400	0.415	0.475	0.482	0.485
F	t (min)	690	486	289	265	239
	MR	0.223	0.242	0.284	0.288	0.291
TDT* (min)		1090	1015	680	588	515

*Total drying time

Table 5. Drying air parameters and duration of each drying segment in the proposed drying regime.

Eksperiment	Segment				
	I (OC)	II (CD)	III (DE)	IV (EF)	V
6	Ekps. 1	Eksp. 2	Eksp. 4	Eksp. 5	70^{0}C / 45%
Segment duration (min)	200	89	43	87	140

The "upper critical" point D, in the proposed drying regime, was reached after 289 min. If this value is compared with the corresponding value taken from the simulated drying curve of the German model it can be seen that is higher. This result was expected and is related with values of the drying air humidity. In the second case drying air humidity was 10% higher at the beginning of the drying. The main functions in the first segment of the proposed drying regime was to restrain the moisture transport (evaporation), through the boundary layer between material surface and the bulk air, and to heat the ceramic body to the temperature of the drying air. That is the reason why higher values of the drying air humidity in the first segment were selected. First drying section was over after 332 min. This value is similar to the corresponding value obtained from the German model. It is also expected result which is correlated with the reduction rate of the drying humidity up to the value applied in the second drying segment of the proposed drying regime. Drying was over after 570 min. This value is lower than the corresponding value obtained using the German model. This is also expected result since the simultaneous adjustment of the drying air parameters has started 100 minutes earlier. Physico-mechanical data are in accordance with the history of drying. All values are lower if the tested samples were previously dried according to the second drying procedure. It is important to mention that the flexural strength as well as twist and camber coefficients were higher than the allowed values defined in the norms EN 1304.

Table 6. Flexural strength of the dried and fired samples.

Average results related to the samples which were previously dried using the	DS (kN)	FS (kN) 1050^0C
I - procedure	0.75	1,90
II - procedure	0.84	2.47
Criteria is defined in EN 1304	Minimal allowed flexural strength	
	0.73	1.2

Table 7. Regularity of shape - twist and cambers coefficients.

Average results related to the samples which were previously dried using the	Twist coefficient TC (%)	Cambers coefficient R (%)	
		Longitudal	Transverse
I - procedure	0.89	0.90	1.05
II - procedure	0.48	0.51	0.57
Criteria is defined in EN 1304 (Tables 1 – 3)	Allowed deviation for C and R		
	$\leq$ 2%	$\leq$ 2%	$\leq$ 2%

4. Conclusions

The procedure for setting up the non isothermal drying regime was compared with the one reported by the German group of authors in 2008. Using the instructions provided within the published articles a model for drying simulation according to the German method was firstly designed. After that both procedures were applied on the same clay raw material. Results have shown the absence of cracks on dried and fired samples. The time period to reach "upper critical" point was lower in the case of the German method. First drying section was nearly the same for both methods. Total drying time was higher in the case of German method. Physico-mechanical data were in accordance with the proposed drying regimes. All values are lower if the tested samples were previously dried according to the second procedure. Presented results have additionally validated that the second dying model can be used for the accurate prediction of industrial drying kinetics and a reliable estimation of moisture transport during drying.

Acknowledgement

This paper was realized under the project *ИИИ* 45008 which was financed by ministry of education and science of Serbia.

5. References

[1] Vasić M, Grbavčić Ž and Radojević Z 2014 Analysis of Moisture Transfer During the Drying of Clay Tiles with Particular Reference to an Estimation of the Time-Dependent *Effective Diffusivity Drying Technology* **32**(7) 829-840
[2] Junge K, Telljohann U and Deppe D Drying of green bricks Capillarity and pore volume as essential criteria for the transport process of water and dissolved salts *Ziegel Ind. International* **8** 39-51
[3] Cranck J 1975 *The Mathematics of Diffusion* (Oxford University Press: New York)
[4] Silva D P W, Silva S P D M C, Silva S P D D, Silva S P D C 2008 Numerical simulation of the water diffusion in cylindrical solids *Int. Jour of food Eng.* **2** 1-16
[5] Efremov G and Kudra T 2004 Calculation of the Effective Diffusion Coefficients by Applying A Quasi-Stationary Equation for Drying Kinetics *Drying Technology* **22**(10) 2273-2279
[6] Luikov A V 1975 System of differential equations of heat and mass transfer in capillary-porous bodies (review) *Int. Jour. of heat and Mass Transfer* **18**(1) 1-14
[7] Hashimoto A, Stenstrom S and Kameoka T 2003 Simulation of convective drying of wet porous materials *Drying Technology* **21**(8) 1411-1431
[8] Whitaker S 1998 Coupled transport in multiphase systems: A theory of drying *Adv. in Heat Transfer* **31** 1-104
[9] Kowalski S J 2000 Toward a thermodynamic of drying process *Chem. Ing. Sciences* **55** 1289-1304
[10] Yiotis A G, Tismpanogiannis I N, Stubos A K, Yortsos Y C 2006 Pore network study of the characteristic periods in the drying of porous materials *Jour of Colloid and Interface Sci.* **297** 738-748
[11] Telljohann U and Junge K 2008 Moisture diffusion coefficients for modeling the first and second drying section of green bricks *Drying Technology* **26**(7) pp 855-863
[12] Junge K and Tretau A Increasing the efficiency of drying plants through the use of modern low-energy dryers 2007 *Ziegel Ind. International* **9** 22-31
[13] Vasić M and Radojević Z 2016 Setting up the drying regimes based on the theory of moisture migration during drying *IOP Conf. Series: Materials Science and Engineering* **145**
[14] Vasić M, Rekecki R Radojević Z 2018 A procedure for setting up the drying regime that is consistent with the nature and properties of clay raw material *Drying Technology* **36**(3) 267-282
[15] Rekecki R and Ranogajec J 2008 Design of ceramic miscrostructures based on waste materials *Proc. and Appl. of Ceramic* **2** 89-95
[16] Vasić M, Rekecki R and Radojević Z 2017 Defining a procedure for predicting the duration of the approximately isothermal segments within the proposed drying regime as a function of the drying air parameters *IOP Conf. Series: Materials Science and Engineering* **227**